

# Mechanisms Determining the Time Course of Secretion in Neuroendocrine Cells

Robert H. Chow,<sup>\*†</sup> Jurgen Klingauf,<sup>\*</sup>  
Christian Heinemann,<sup>\*</sup> Robert S. Zucker,<sup>‡</sup>  
and Erwin Neher<sup>\*</sup>

<sup>\*</sup>Max Planck Institute for Biophysical Chemistry  
Department of Membrane Biophysics  
Hermann-Rein-Str. #3  
D-37075 Goettingen  
Germany

<sup>†</sup>Max Planck Institute for Experimental Medicine  
Department of Molecular Biology of Neuronal Signaling  
Am Fassberg  
D-37077 Goettingen  
Germany

<sup>‡</sup>Department of Molecular and Cell Biology  
University of California  
Berkeley, California 94720

## Summary

Transmitter release from chromaffin cells differs from that in synapses in that it persists for a longer time after  $\text{Ca}^{2+}$  entry has stopped. This prolonged secretion is not due to a delay between vesicle fusion and transmitter release, nor to slow detection of released substance: step increases in capacitance due to single vesicle fusion precede the release detected by amperometry by only a few milliseconds. The persistence of secretion after a depolarization is reduced by addition of mobile calcium buffer. This suggests that most of the delay is due to diffusion of  $\text{Ca}^{2+}$  between channels and release sites, implying that  $\text{Ca}^{2+}$  channels and secretory vesicles are not colocalized in chromaffin cells, in contrast to presynaptic active zones.

## Introduction

In both neuroendocrine cells and neurons, regulated secretion is triggered by an elevation of cytoplasmic  $[\text{Ca}^{2+}]_i$  (Douglas, 1968; Katz, 1969). Yet, investigators have long suspected that the details of secretion regulation differ in these two classes of cells, perhaps due to the different vesicle types—primarily dense core in neuroendocrine cells and small clear vesicles in neurons (de Camilli and Jahn, 1990; Verhage et al., 1991).

In chromaffin cells, secretion persists for tens of milliseconds after  $\text{Ca}^{2+}$  entry through voltage-gated  $\text{Ca}^{2+}$  channels has ceased (Chow et al., 1992). In contrast, secretion at neuronal synapses terminates within a few milliseconds after the cessation of  $\text{Ca}^{2+}$  entry (Katz, 1969; Augustine et al., 1985). The persistence of secretion in chromaffin cells is not due to slow kinetics of the secretory machinery, as was shown when caged- $\text{Ca}^{2+}$  photolysis was used to elicit secretion (Heinemann et al., 1994), which was monitored as increases in the cell membrane capacitance (Lindau and Neher, 1988).

Two plausible explanations for the persistence of secretion in chromaffin cells are, first, that the release of transmitter from vesicles follows exocytotic fusion after a delay and, second, that calcium channels and vesicles

are not colocalized—which would lead to a diffusional lag between  $\text{Ca}^{2+}$  entry and its action. The second idea is supported by previous estimates of the level of  $[\text{Ca}^{2+}]$  “seen” by secretory granules in adrenal chromaffin cells during short depolarizations (Chow et al., 1994). Using the secretory apparatus as a “bioassay” for the calcium level, we estimated that the  $[\text{Ca}^{2+}]$  triggering exocytosis peaks at  $<10 \mu\text{M}$ , during 20 ms depolarizations. Such peak levels are lower than expected for the case of colocalization of vesicles and  $\text{Ca}^{2+}$  channels with a separation of 20–50 nm (Yamada and Zucker, 1992; Roberts, 1994). On the other hand, these levels would be appropriate for mean separations of 100–200 nm. For such separation distances,  $\text{Ca}^{2+}$  buffers would be expected to have a significant impact on the  $[\text{Ca}^{2+}]$  attained at the vesicles.

For this paper, we investigated how  $\text{Ca}^{2+}$  buffers influence the time course of secretion after a depolarization. Upon termination of a depolarization, the  $\text{Ca}^{2+}$  concentration gradient near  $\text{Ca}^{2+}$  channels is expected to collapse due to ion redistribution. The rate at which secretion decays away is expected to reflect the speed of this gradient collapse, and it is expected to be influenced by  $\text{Ca}^{2+}$  buffering—particularly if the channels and the vesicles are not colocalized. Our results affirm the importance of both immobile and mobile buffers in determining the  $[\text{Ca}^{2+}]$  time course.

To examine whether there is a delay between vesicle fusion and catecholamine release, we used membrane capacitance measurements to monitor the time of vesicle fusion, and we simultaneously measured catecholamine release with the electrochemical method of amperometry. In our experimental conditions (see Experimental Procedures), the fusion of a chromaffin cell granule should appear immediately as an increment in the whole-cell capacitance (assuming an initial fusion pore conductance of 250 pS, approximately the size previously measured for fusing mast-cell vesicles [Almers, 1990]). Our results demonstrate that detection of transmitter release with amperometry occurs with a delay of only a few milliseconds after vesicle fusion—not sufficient to account for the many amperometric events that occur long after a depolarization has ended.

We conclude that three sources of delay account for most, if not all, of the persistence of secretion after a depolarization in neuroendocrine cells: first, the submembrane  $[\text{Ca}^{2+}]$  time course, which determines the major part of the delay and which reflects the distance separating the vesicles from  $\text{Ca}^{2+}$  channels and the degree of  $\text{Ca}^{2+}$  buffering by both fixed and mobile buffers; second, the kinetics of  $\text{Ca}^{2+}$  action at the secretory apparatus; and third, the finite time between vesicle fusion and detection of intravesicular content release.

## Results

### Comparison of Capacitance and Amperometric Time Courses for Step Depolarizations

We monitored secretion using simultaneous amperometry and capacitance measurements, while stimulating

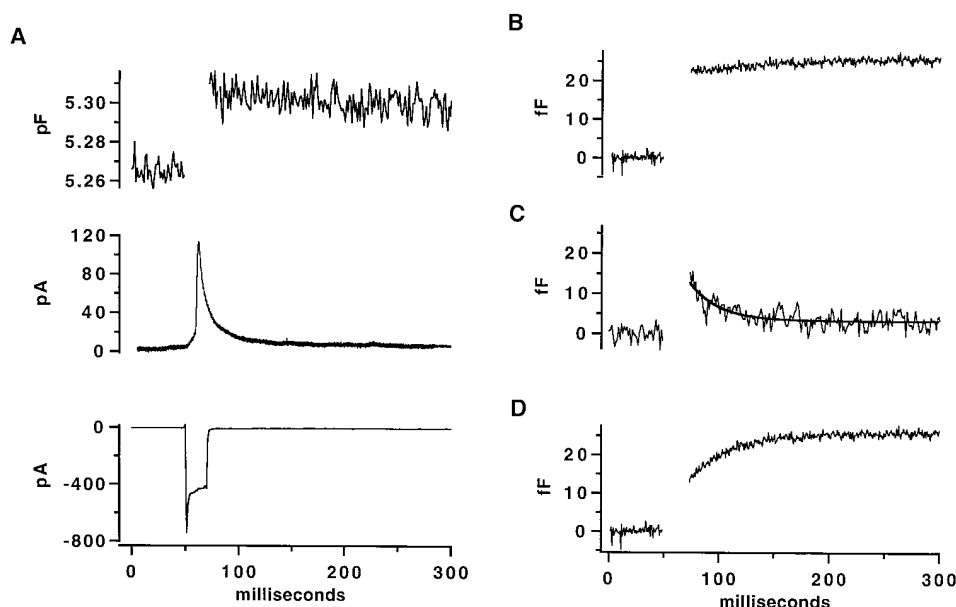


Figure 1. Depolarizations Evoke  $\text{Ca}^{2+}$  Current and Secretion Detectable by Amperometry and Capacitance Measurements

(A) Single 20 ms step depolarization elicits  $\text{Ca}^{2+}$  current, an increase in membrane capacitance, and an amperometric event. Simultaneous recording of membrane capacitance (top trace), single amperometric event (middle trace), and the whole-cell  $\text{Ca}^{2+}$  current (bottom trace) in response to a 20 ms step depolarization.

(B) Averaged capacitance records (265 depolarizations) for traces early in experiments for 4 cells.

(C) Averaged capacitance records (26 depolarizations) for traces late in experiments. A single exponential fit (smooth line) having a time constant of 23.6 ms is superimposed on the averaged record.

(D) Difference record to show the corrected capacitance time course. The fitted curve in (C) was subtracted from (B). After correction, the capacitance trace shows that secretion continues for a period after the end of the depolarization.

cells in the whole-cell configuration with 20 ms step depolarizations at 0.2 Hz. Note that, at this frequency of stimulation, the  $[\text{Ca}^{2+}]$  between depolarizations does not return to basal but attains levels of around 500 nM (as assessed by Fura-2 measurements, data not shown). This leads to a sizable pool of release-ready vesicles (Neher and Zucker, 1993; von Rüden and Neher, 1993). An example of the capacitance record for a single stimulus is shown in Figure 1A (top trace), along with the simultaneously recorded amperometric event (middle trace) and the  $\text{Ca}^{2+}$  current trace (bottom trace).

Using depolarizing steps to stimulate secretion leads to several artifacts in the capacitance record that make difficult a comparison of the time courses of secretion determined from amperometry and capacitance. First, capacitance measurements are not valid during step depolarizations, owing to opening of voltage-gated channels (Lindau and Neher, 1988). Furthermore, immediately following depolarizations, there is a decaying capacitive transient ( $\Delta C_i$ ), unrelated to secretion, which has previously been related to sodium channel gating-current relaxation (Horrigan and Bookman, 1994). These two artifacts occur during the period critical for the comparison of capacitance and amperometric time courses. To contend with these problems, we used short (20 ms) depolarizations, and we attempted to correct for  $\Delta C_i$ . The latter correction involved selecting and averaging the capacitance records showing little or no secretion, typically 20–30 min into a whole-cell recording, by which time critical secretory components have “washed out” (Augustine and Neher, 1992). At such late times,  $\Delta C_i$  is

still present, as illustrated in Figure 1C (average of 26 traces), which shows a capacitance transient following a gap (period during which the depolarization made capacitance calculation invalid). The transient decays within a few tens of milliseconds to a small maintained level (about 4 fF in Figure 1C). The record is reasonably well fitted with a decaying single exponential that has a time constant of 23.6 ms (solid line superimposed).

The decaying capacitance transient is not likely to be due to endocytosis at such late times in the recordings, as most endocytosis “washes out” over a few minutes after establishing the whole-cell configuration in bovine chromaffin cells (Burgoyne, 1995). Furthermore, in separate experiments on 8 cells, we recorded similar transients in  $\text{Ca}^{2+}$ -free solutions and confirmed that they are unrelated to secretion (data not shown), as noted previously by Horrigan and Bookman (1994). The mean decay time constant was  $16 \pm 5$  ms, with a range from 9 to 25 ms.

The fitted curve was then subtracted from the average of traces that were recorded early in the experiments and that show clear secretion (Figure 1B, average of 265 traces), to reconstruct the time course starting immediately after a step depolarization. As shown in Figure 1D, the corrected time course shows a clear rising phase, lasting tens of milliseconds after the depolarization, whereas the noncorrected average record appears almost flat on this time scale. We do not mean to imply that, after the correction procedure, secretion has exactly the time course shown in Figure 1D. The contamination of the capacitance record by endocytosis is still

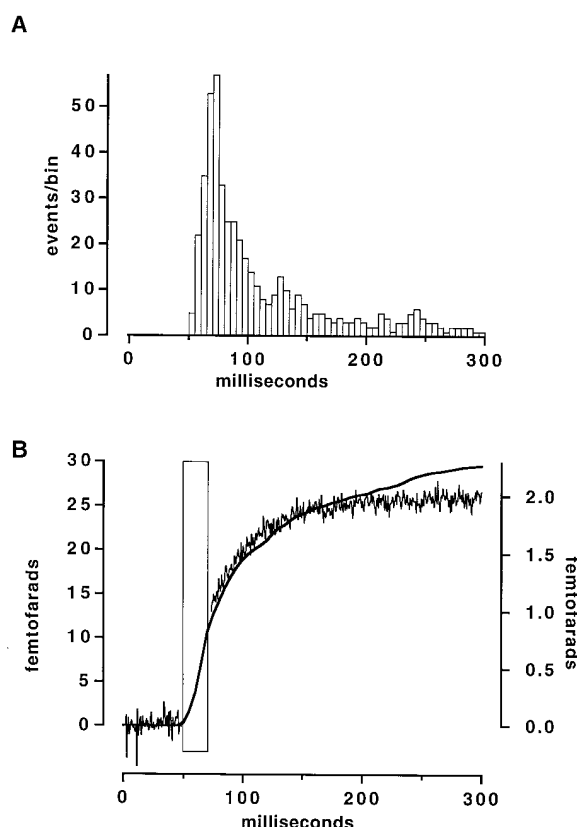


Figure 2. Comparison of Cumulative Amperometric and Capacitance Measurements of Secretion

(A) Composite amperometric latency histogram for repeated 20 ms depolarizations for 4 cells (same cells as for Figure 1B). The latency is defined as the time between the start of the depolarization and the beginning of an amperometric event (Chow and von Rüden, 1995).

(B) Integrated amperometric latency histogram superimposed on the corrected capacitance time course (Figure 1D). The latency histogram was integrated to obtain a cumulative record of secretion for comparison with the capacitance trace. The traces are superimposed after the integrated latency histogram (smooth line) has been divided by the number of depolarizations (265), multiplied by 2.5 fF per event to convert to units of capacitance, and then scaled to match the amplitude of the capacitance record at 80 ms after the end of the depolarization, when the capacitance transient related to channel gating has subsided. After the scaling, it can be seen that the carbon fiber has detected ~8% of the total events contributing to the capacitance increase. The period of depolarization is indicated by the boxed area. The scale to the left refers to the capacitance record, and the scale to the right to the scaled integrated latency histogram.

an unresolved problem, which becomes significant late in depolarization records. Nevertheless, as shown below, after correction the capacitance measurements give results compatible and consistent with the amperometric data.

Figure 2A shows the amperometric latency histogram from the same cells used for Figure 1. To obtain the cumulative time course of secretion from this figure for comparison with the capacitance record, the histogram was integrated. Finally, time courses of secretion determined by amperometry and by capacitance were superimposed for comparison in Figure 2B, after scaling the

Table 1. Internal Recording Solutions

	A	B	C <sup>a</sup>	D
Cs-Glu	145	145	145	145
Cs-HEPES	10	10	10	10
NaCl	8	8	8	8
GTP	0.3	0.3	0.3	0.3
Mg-ATP	2	2	2	2
MgCl <sub>2</sub>	1	1	1	1
CaCl <sub>2</sub>	—	9.83	—	.73
Fura-2	0.1	0.1	—	0.1
EGTA	—	10	—	1.2

<sup>a</sup> Mg may have been removed by Chelex treatment. See Experimental Procedures.

amplitudes of each to match 80 ms after the end of the depolarization, when the non-secretion-related capacitance transient is over (about three times the time constant of the nonsecretion capacitance transient). Both time courses after the depolarization gap are remarkably similar, although at late times they diverge, presumably due to the onset of endocytosis. The amperometric time course may have a delay of about 5 ms compared with the corrected capacitance time course during the initial phase. The actual delay, however, is difficult to ascertain accurately by this approach and will vary depending upon exactly how the amperometric curve is scaled relative to the capacitance trace.

### Cross-Correlation of Single Secretory Events in Amperometry and Capacitance

To refine the comparison between the time of vesicle fusion and transmitter release, we correlated individual secretory events as assayed by amperometry and capacitance measurements. Cells were perfused in the whole-cell configuration with a solution (Table 1, solution B) for which the free  $[Ca^{2+}]$  was buffered to 10  $\mu M$  to stimulate secretion, and capacitance and amperometric signals were monitored in parallel. As illustrated in Figure 3A, with large amperometric events, it was sometimes possible to see a nearly simultaneous "step" in the capacitance record. In this case, the amperometric event follows the increment in capacitance after a lag of 1.5 ms.

For most events, however, the signal-to-noise ratio in the capacitance record did not permit us to resolve the expected step increases in capacitance. To enhance the signal-to-noise ratio, we used a signal-averaging approach. Amperometric signals were identified and used to select segments from the capacitance traces recorded in parallel. The selected capacitance traces were then averaged, after being aligned at the time of onset of the amperometric signals.

Figure 3B shows the signal obtained by averaging 60 capacitance sweeps (from a single cell) that have been aligned at the beginning of the amperometric events. In this time-locked average capacitance record, there is a clear step that is absent in a randomly aligned capacitance record (Figure 3C, composed of the same number of sweeps and from the same cell as Figure 3B). Figure 3D shows the capacitance step at higher time resolution.

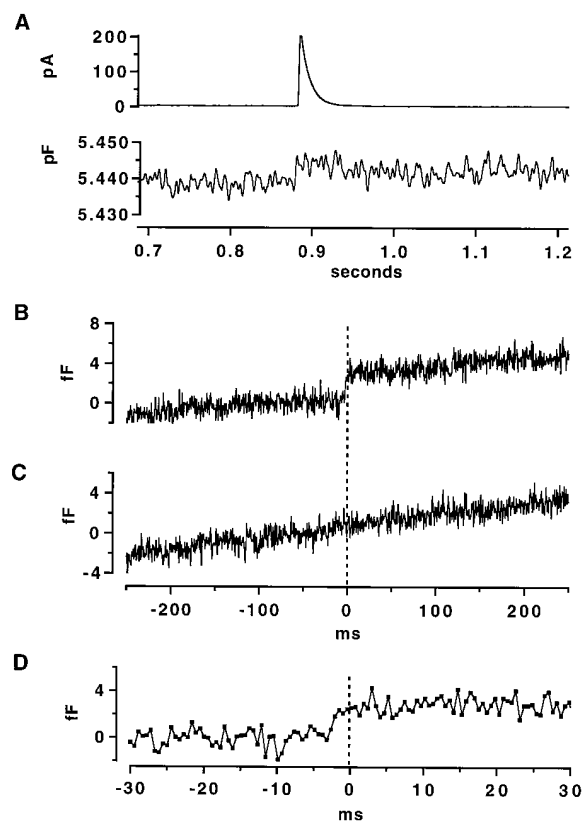


Figure 3. Cross-Correlation of Capacitance Steps and Amperometric Events

(A) Correlation between a single amperometric event and a step in the capacitance record during whole-cell dialysis with a high  $[Ca^{2+}]_i$  solution. Although the signal-to-noise ratio in whole-cell recordings does not usually permit it, one can occasionally resolve the capacitance step associated with an individual amperometric event. The capacitance trace has been digitally filtered once using a binomial smoothing algorithm.

(B) Averaged capacitance records (60 traces) from a single cell, aligned at the time of onset of amperometric signals (defined to be time = 0 ms).

(C) Averaged capacitance records from the same sweeps as in (B) but with random alignment.

(D) Same trace as in (B) but at higher time resolution to illustrate the delay between the onset of the amperometric events relative to the rise in capacitance.

The capacitance starts to rise 3–5 ms prior to the beginning of the amperometric signals and is >90% of its final level by the time the amperometric signal begins. The midpoint of the capacitance step occurs about 2.3 ms before the start of the amperometric signal. The mean amplitude of the 60 averaged events was approximately 2.7 fF, as expected (Neher and Marty, 1982). Similar results were obtained in another 9 cells. It should be noted that we made an effort (see Experimental Procedures) to align the capacitance records with respect to the very beginning of foot signals, if present. Thus, the capacitance rise precedes the amperometric current by a few milliseconds.

#### Latency Histogram Time Course Is Influenced by $Ca^{2+}$ Buffers

Neher and Augustine (1992) showed that bovine chromaffin cells have significant amounts of endogenous

fixed (nonmobile)  $Ca^{2+}$  buffers. Subsequently, Zhou and Neher (1993) showed that there may be, in addition, endogenous mobile  $Ca^{2+}$  buffers in these cells. In mixtures of fixed and mobile buffers, the time course of  $[Ca^{2+}]$  transients is expected to be highly dependent on the relative amounts of each (Nowycky and Pinter, 1993) and on the distance between vesicles and  $Ca^{2+}$  channels (Roberts, 1994). Fixed buffers alone tend to prolong  $[Ca^{2+}]$  transients. Addition of mobile buffers to fixed buffers leads to speeding up the transients and more rapid collapse of gradients, as the mobile buffers compete with fixed buffer for calcium and transport it away from the sites of  $Ca^{2+}$  entry. We have therefore tested the effects of removing or elevating mobile  $Ca^{2+}$  buffers on the decay of the amperometric latency histograms after the end of depolarizing stimuli.

Experiments were performed as described above for Figure 1, but in a paired fashion, alternating cells being dialyzed with "standard" internal solution (Table 1, solution A) and those with "test" solutions containing differing amounts of  $Ca^{2+}$  buffers (see Experimental Procedures). Recordings were rejected if the access resistance increased to greater than 10 M $\Omega$ . The decay of the amperometric latency histograms after depolarizations was fit with single exponentials to allow comparison of the decay rates in different conditions (we do not imply any theoretical basis for a single-exponential decay). Latency histograms for the standard solutions had decay time constants consistently between about 16 and 18 ms.

#### Buffering with 100 $\mu M$ Fura-2 ("Standard" Conditions)

Figure 4A shows a composite amperometric latency histogram for repeated 20-millisecond step depolarizations in 9 cells. In these experiments, the cells were perfused with solution A (Table 1), our standard internal solution, which contains 100  $\mu M$  Fura-2. During the step depolarization,  $Ca^{2+}$  currents were activated, stimulating a progressive increase in the rate of secretion, which is reflected in the climb in the number of events in the latency histograms. Upon repolarization, however, the secretory rate decayed gradually to near 0. The decay of the histogram has been fitted with a single exponential having a time constant of 17 ms.

#### No-Added Calcium Buffer

In the experiment of Figure 4B, we have patch-clamped chromaffin cells in the whole-cell configuration with pipette solutions containing neither Fura-2 nor other diffusible  $Ca^{2+}$  buffers (except ATP, which, owing to its low  $Ca^{2+}$  affinity, should have little influence). The pipette solutions (Table 1, solution C) have been filtered through a bed of Chelex to remove free divalents, and Chelex beads were put in the patch pipette to chelate any divalent ions released from the glass. Endogenous mobile  $Ca^{2+}$  buffer should dialyze out of the cell within 100–200 s (Zhou and Neher, 1993), leaving only fixed agents to buffer  $Ca^{2+}$  transients. The decay of the amperometric latency histogram has a time constant of about 30 ms—much slower than the decay in standard conditions. This is in accord with the idea that fixed buffers alone should prolong  $[Ca^{2+}]$  transients, as discussed above.

#### High Buffer Capacity

Figure 4C shows the effect of increasing the concentration of (exogenous) mobile buffer, in the form of Fura-2 and EGTA. To ensure that we could measure secretion,

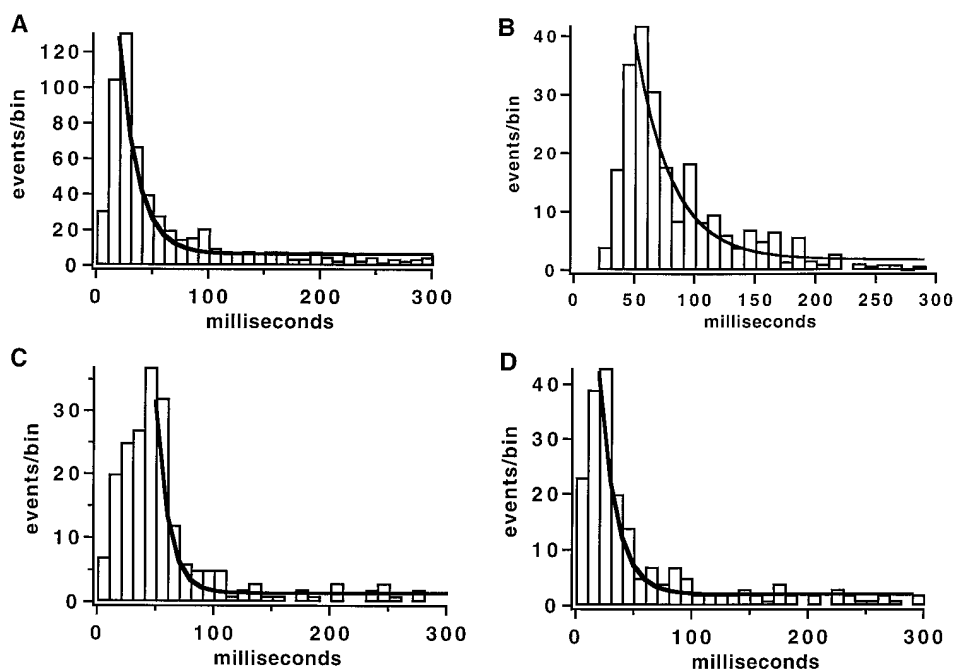


Figure 4. The Effect of Varying Concentration of Mobile  $\text{Ca}^{2+}$  Buffer on Secretory Latencies

(A) Composite amperometric latency histogram from 9 cells, 100  $\mu\text{M}$  Fura-2. This latency histogram was compiled from 9 cells, subjected to repeated 20 ms depolarizations. After the end of the depolarization, the histogram decays away with a time constant of  $\sim 17$  ms.

(B) Composite amperometric latency histogram for 2 cells with no exogenous  $\text{Ca}^{2+}$  buffer. This experiment was performed as in (A), except that the pipette solution was first filtered over Chelex beads to remove free  $\text{Ca}^{2+}$  and several Chelex beads were included in the pipette to minimize the effects of divalents leaching from the pipette glass. The frequency of events decays away after the end of the depolarization with a time constant of  $\sim 30$  ms.

(C) Composite latency histogram for 7 cells perfused with an internal solution containing 1.2 mM EGTA in addition to 100  $\mu\text{M}$  Fura-2. The pulse length was 50 ms, instead of the standard 20 ms for these experiments, because 20 ms pulses did not elicit sufficient release in these conditions. The frequency of events decays away after the depolarization with a time constant of about 10.8 ms.

(D) Composite latency histogram for 5 cells patched with nystatin in the perforated-patch configuration. The frequency of events decays away after the depolarization ends with a time constant of about 16 ms.

despite such high buffer capacity, we designed the solutions to have a nominal free  $[\text{Ca}^{2+}]$  of 300 nM (Table 1, solution D). Despite this, the probability of recording an amperometric event per depolarization was decreased to about 0.2, compared with about 1.3 in our standard solution (Table 1, solution A). The decay time constant of the latency histogram is reduced by nearly half compared with Figure 4C.

#### Nystatin

In these experiments, we hoped to study the effect of only endogenous buffers, both mobile and fixed, on the decay of the latency histogram following depolarizations. Recordings were made using Nystatin to perforate the membrane patch, without loss of intracellular constituents. Figure 4D shows the resulting latency histogram for 4 cells. The decay of secretion after the termination of the depolarization has a time constant of  $\sim 17$  ms, similar to what is found with 100  $\mu\text{M}$  Fura-2 in the pipette (Figure 4A). This suggests that the endogenous  $\text{Ca}^{2+}$  buffers have about the same effect on the  $\text{Ca}^{2+}$  time course as 100  $\mu\text{M}$  Fura-2, included in a patch pipette.

#### Discussion

##### Secretion Assayed by Capacitance and Amperometry Compared

In previous experiments on secretion triggered by short step depolarizations, we were puzzled by the finding that

the capacitance increase apparently ceased as soon as the depolarization ended, whereas amperometric events continued for many tens of milliseconds (Chow et al., 1992). We have found that the discrepancy can be attributed to the nonsecretion capacitive transient,  $\Delta C_i$ , that has been described by Horrigan and Bookman (1994). After correction for  $\Delta C_i$ , the capacitance time course and the integrated amperometric time course rise nearly in parallel during the early phase after a depolarization. There may be a small delay between the two time courses, but the magnitude of the delay cannot be determined accurately by this type of experiment.

An additional complication is the superimposition of endocytosis in the capacitance records, especially at late times ( $>50$ – $100$  ms) after a stimulus. Endocytosis is not seen consistently after depolarization-induced secretion, and it occurs at variable rates. However, by comparing the time course of the averaged capacitance record and the integrated amperometric histogram, one can get a rough idea of the contribution of endocytosis to the capacitance trace. Figure 2B shows that, after an initial phase of nearly parallel time course, the capacitance record and the integrated amperometric histogram diverge, due to the onset of endocytosis. At 250 ms after the end of the short depolarization, the capacitance record is approximately 13% less than the integrated amperometric histogram. This corresponds to a time constant for membrane retrieval of  $\sim 1.8$  s, if the cell were

ultimately to retrieve the same amount of membrane as was added during the depolarization. This rate of retrieval is similar in magnitude to rates previously reported in chromaffin cells (Burgoyne, 1995) and melanotrophs (Thomas et al., 1994).

The cross-correlation experiments (Figure 3) showed clearly that the capacitance increase due to vesicle fusion is followed within only a few milliseconds by the release of transmitter. This implies that a significant fraction of the catecholamine within secretory granules must be freely diffusing or rapidly released from a storage matrix. On the other hand, a delay of onset in the amperometric current of 3–5 ms is more than can be attributed simply to diffusion of the transmitter from the cell surface to the carbon-fiber detector (a distance of  $<1\ \mu\text{m}$ ) and may be due to the early fusion pore having a short-lived state that does not conduct any transmitter, or that conducts too little to be detected with our carbon-fiber electrodes. In addition, the cross-correlation experiments showed that the mean capacitance step is  $\sim 2.7\ \text{fF}$ , in good agreement with previous measurements made in the cell-attached configuration (Neher and Marty, 1982). This capacitance step is the size expected for vesicles that have a mean diameter of about 280 nm assuming a specific capacitance of  $1\ \mu\text{F}/\text{cm}^2$ , close to the mean diameter of chromaffin granules previously determined morphometrically (Coupland, 1968).

#### $\text{Ca}^{2+}$ Buffering in Bovine Chromaffin Cells

Neher and Augustine (1992) and Zhou and Neher (1993) measured the  $\text{Ca}^{2+}$  binding ratio of bovine chromaffin cells: for every 42  $\text{Ca}^{2+}$  ions that enter the cytoplasm, 41 ions are bound rapidly to endogenous  $\text{Ca}^{2+}$  buffers, and 1 ion remains free. Most of the buffers are apparently fixed or nonmobile. However, there is a component of slowly mobile  $\text{Ca}^{2+}$  buffer in some cells, having a  $\text{Ca}^{2+}$ -binding ratio of about 10 (Zhou and Neher, 1993). Furthermore, the authors noted that a component of rapidly mobile  $\text{Ca}^{2+}$  buffer, having a binding ratio of up to 7, could be present, although they could not detect it, owing to limitations of their approach.

Our experiments showed that, in the absence of added exogenous mobile buffer, secretion decayed away more slowly after a depolarization than it did in the presence of 100  $\mu\text{M}$  Fura-2. This agrees with there being substantial fixed  $\text{Ca}^{2+}$  buffer, which slows the collapse of  $[\text{Ca}^{2+}]$  gradients after a depolarization. Mobile buffer competes with the fixed buffer and transports bound  $\text{Ca}^{2+}$  away from the sites of entry. The finding that the rate of secretory decay with nystatin (which should preserve endogenous buffering) is nearly the same as with whole-cell recording with 100  $\mu\text{M}$  Fura-2 means that there are endogenous mobile buffers with a buffer capacity similar to that of 100  $\mu\text{M}$  Fura-2.

Photometrically measured  $[\text{Ca}^{2+}]$  at the end of a depolarization with 100  $\mu\text{M}$  Fura-2 is typically  $\sim 1\ \mu\text{M}$ . The  $\text{Ca}^{2+}$ -binding ratio  $\kappa_B$  is given by the equation (see Zhou and Neher, 1993):

$$\kappa_B = \frac{[\text{B}]_t/K_d}{(1 + [\text{Ca}^{2+}]_t/K_d)^2}$$

where  $[\text{B}]_t$  is the total buffer concentration and  $K_d$  is the

dissociation constant of the buffer. If we assume that the  $K_d$  of Fura-2 is 238 nM (Zhou and Neher, 1993), the  $\text{Ca}^{2+}$ -binding ratio of 100  $\mu\text{M}$  Fura-2 would be approximately 15—larger by a factor of 2 than the upper limit for highly mobile  $\text{Ca}^{2+}$  buffer given by Zhou and Neher (1993). This would, however, be an overestimate of the buffering capacity at the secretion sites, as our  $[\text{Ca}^{2+}]$  measurements with Fura-2 give a cell-averaged value, which is significantly lower than that near the membrane and channels (Augustine and Neher, 1992; Chow et al., 1994). Thus, a submillimolar concentration of low-molecular-weight  $\text{Ca}^{2+}$ -binding molecule with high  $\text{Ca}^{2+}$  affinity would have the buffer capacity and properties appropriate to give the measured  $[\text{Ca}^{2+}]$  time course.

#### Secretion in Chromaffin Cells and in Synapses: Mechanisms Underlying Differences in Time Course

As noted in the Introduction, secretion from chromaffin cells differs from that in most neuronal synapses in that it persists for a longer time after  $\text{Ca}^{2+}$  entry has stopped. The difference may be related to the different vesicle types. This point has been recently emphasized by a study using carbon-fiber amperometry in leech neurons (Bruns and Jahn, 1995). These cells contain serotonin, a readily oxidizable transmitter, in both dense-core and small synaptic vesicles. Interestingly, the latency histogram for dense-core vesicle exocytosis is significantly delayed compared with exocytosis of small synaptic vesicles.

We have examined possible mechanisms for the delayed secretion. Most, if not all, of the observed delay can be accounted for by a combination of several factors: first, the submembrane  $[\text{Ca}^{2+}]$  time course at the vesicle fusion machinery, which should be determined by the distance separating the vesicles from  $\text{Ca}^{2+}$  channels and by the degree of  $\text{Ca}^{2+}$  buffering, both by fixed and by mobile buffers; second, the kinetics of  $\text{Ca}^{2+}$  action at the secretory apparatus; and third, the finite time between vesicle fusion and the onset of intravesicular content release.

The delay between vesicle fusion and detection of transmitter release is only a few milliseconds—too small to account fully for the tens of milliseconds over which secretion persists after a depolarizing stimulus ends. The rate at which the secretory machinery is capable of turning off is also very fast, and could account for at most  $\sim 3\ \text{ms}$  of delayed secretion (Heinemann et al., 1994). Thus, it appears that the most important mechanism for the delayed secretion is the prolonged time course of the  $\text{Ca}^{2+}$  reaching the fusion machinery (see also Chow et al., 1994). The slow time course is compatible with separation of the secretory vesicles from the calcium channels by distances on the order of 100–200 nm (Roberts, 1994). Furthermore, as we have shown,  $\text{Ca}^{2+}$  buffering can influence the time course. The net effect depends upon the exact proportion of fixed to mobile buffer and may also depend upon the spatial distribution of the buffering relative to the secretory vesicles and calcium channels.

The normal stimuli for secretion in chromaffin cells are action potentials, triggered by sympathetic nerve

endings. If  $\text{Ca}^{2+}$  channels and vesicles are not strictly colocalized, then the small amount of  $\text{Ca}^{2+}$  that enters during a single isolated action potential may not be sufficient to trigger significant secretion, especially given the strength of endogenous  $\text{Ca}^{2+}$  buffers. On the other hand, with trains of action potentials the injected  $\text{Ca}^{2+}$  should build up to levels sufficient to trigger secretion. This is supported by the observation that  $\text{Ca}^{2+}$ -channel tail currents alone do not elicit significant secretion from these cells (Chow and von Rüden, unpublished data). Furthermore, Zhou and Mislér (1995) have recently demonstrated that single action potentials only infrequently elicit secretion, as monitored by a carbon-fiber electrode, whereas trains of action potentials are highly effective in eliciting secretion. Interestingly, at low frequencies of stimulation, the few observed amperometric events were closely coupled in time to the action potentials, whereas for higher frequencies, there was a progressive "desynchronization." This is exactly what would be expected if with low frequency firing  $\text{Ca}^{2+}$  were confined to the immediate vicinity of single  $\text{Ca}^{2+}$  channels or channel clusters, whereas at higher frequencies of firing,  $\text{Ca}^{2+}$  were elevated globally, leading to fusion of vesicles from a larger docked vesicle pool. Synchronization between action potentials and secretion is lost in this case, because global elevation persists for seconds or even tens of seconds.

## Experimental Procedures

### Cell Preparation and Whole-Cell

#### Patch-Clamp Recording

Chromaffin cells from bovine adrenal glands were prepared and cultured as described by Zhou and Neher (1993). Cells were used 1–2 days after preparation. Conventional whole-cell recordings (Hamill et al., 1981) were performed with 2–4 M $\Omega$  pipettes, mounted on the headstage of an EPC-9 patch-clamp amplifier (HEKA, Lambricht, Germany). The membrane potential was held at  $-70$  mV. All experiments were performed at room temperature (21°C–24°C).

### Whole-Cell Capacitance Measurements

Whole-cell capacitance was measured as previously described (Heinemann et al., 1994), combining an EPC-9 patch clamp amplifier and a software lockin system. The stimulus used was a 1600 Hz, 50 mV peak-to-peak sinewave, generated by an ITC-16 data acquisition/pulsing system (Instrutech, Inc., Elmont, NY) operated by a Macintosh Quadra 700 computer running IGOR (Wavemetrics, Lake Oswego, OR) and the Pulse Control XOPs (Jack Herrington and Richard Bookman, Univ. of Miami, Coral Gables, FL).

### Recording Solutions

The external bathing solution for experiments contained 150 mM NaCl, 2.8 mM KCl, 2 mM  $\text{CaCl}_2$ , 1 mM  $\text{MgCl}_2$ , 10 mM HEPES-NaOH, and 2 mg/ml glucose (pH 7.2, 320 mOsm). Patch pipette solutions are listed in Table 1. For the experiments concerning  $\text{Ca}^{2+}$  buffering, differing amounts of  $\text{Ca}^{2+}$  buffer were included in the patch pipettes. In the cases for which no buffer was included, the internal solution (Table 1, solution C) was filtered over a bed of Chelex-100 beads (Bio-Rad Laboratories, Hercules, CA) to remove free  $\text{Ca}^{2+}$ . In addition, Chelex beads were included in the patch pipette to chelate divalent ions that might leach from the glass. This treatment may also have removed  $\text{Mg}^{2+}$ , since Chelex has high affinity for both  $\text{Ca}^{2+}$  and  $\text{Mg}^{2+}$ . For experiments with high  $\text{Ca}^{2+}$  buffer capacity, we added  $\text{Ca}^{2+}$ /Fura-2 or  $\text{Ca}^{2+}$ /EGTA mixtures and calculated "nominal" values of the buffer capacity according to the equations of Zhou and Neher (1993) at a "nominal"  $[\text{Ca}^{2+}]$ . During experiments, however,  $[\text{Ca}^{2+}]$  was elevated above the nominal value due to the repetitive depolarizations, leading to buffer capacities lower than calculated (see Zhou and Neher, 1993). This was not a serious problem,

as the goal was to examine only the qualitative effects of higher or lower  $\text{Ca}^{2+}$  buffer capacity.

### Nystatin Perforated-Patch Recording

Nystatin solutions were prepared as described in Zhou and Neher (1993) at a final concentration of 250  $\mu\text{g/ml}$  (Table 1, solution C). After preparation, the solutions were shielded from light and kept on ice. Patch pipettes were dipped for 10–20 s in nystatin-free solutions, then backfilled with 5  $\mu\text{l}$  of nystatin solution. The remainder of the pipette was filled with nystatin-free solution. The pipettes were immediately mounted in the pipette holder, and a gigaseal to the cell membrane was made within 60 s. Repeated step hyperpolarizations of 10 mV amplitude and 5 ms duration were applied to monitor the progress of membrane permeabilization. Generally, the series resistance decreased to 20 M $\Omega$  or less within 5 min, at which time the experiment was started.

### Carbon-Fiber Electrode Fabrication

Carbon-fiber electrodes were prepared with polyethylene insulation, as previously described (Chow et al., 1992; Chow and von Rüden, 1995). During experiments, the electrodes were backfilled with 3 M KCl solution and mounted on an EPC-7 patch-clamp headstage. A constant voltage of 800 mV (versus an Ag/AgCl bath electrode) was applied to the electrode, whose tip (sensing surface) was pushed gently against the cell surface. The amperometric current was recorded at 1600 Hz, using the same multichannel data acquisition system as was used for capacitance measurements. For experiments in which secretion was elicited by depolarizations, step depolarizations of 20–50 ms duration were used, because they elicit only few amperometric events per depolarization, thus allowing precise determination of the beginning of the isolated signals.

In off-line analysis, a semiautomatic program (written in IGOR macro code) scanned the amperometric data traces, identifying the beginning of each secretory event (the point at which the current exceeded the baseline average plus 2 standard deviations of the noise), and kept a record of the number of events occurring in time bins following the depolarization (the beginning of the depolarization was denoted time = 0). The cumulative record from single cells or multiple cells was used to give latency histograms, as described in Chow et al. 1992, 1994.

### Cross-Correlation Experiments

The goal of these experiments was to compare precisely the time of single-vesicle fusion and the time of catecholamine release. In chromaffin cells, the capacitance "step" due to the fusion of a single vesicle is generally too small to be detected when recording in the whole-cell mode (Neher and Marty, 1982). Thus, it is necessary to perform signal averaging. Cells were patch-clamped in the whole-cell configuration. The pipette contained a solution with free calcium buffered to 10  $\mu\text{M}$  (Table 1, solution B) to stimulate secretion. Near-continuous recording of both capacitance and amperometry was achieved by recording repeated sweeps in tandem, with the ITC-16 multichannel acquisition system. There were short interruptions during the writing of the data to disk. For analysis, the time of the earliest detectable signal ("foot"-signal) was identified for each amperometric event (using the same program as described above for step depolarization experiments), and the capacitance record around the same time period was "cut out" and summed with other cut-out capacitance records, aligned to the beginning of the amperometric event. Further details can be found in the text and legend for Figure 3.

### Acknowledgments

We thank M. Pilot and F. Friedlein for expert technical assistance and preparation of the cells. We thank Drs. Kevin Gillis, Albert Schulte, and Per-Eric Lund for critical feedback on the manuscript. This work has been supported by fellowships to R. H. C. from the Alexander von Humboldt Foundation and the Howard Hughes Medical Institute. R. H. C. is a Howard Hughes Medical Institute Physician Postdoctoral Fellow.

The costs of publication of this article were defrayed in part by the payment of page charges. This article must therefore be hereby

marked "advertisement" in accordance with 18 USC Section 1734 solely to indicate this fact.

Received October 3, 1995; revised November 7, 1995.

## References

- Almers, W. (1990). Exocytosis. *Annu. Rev. Physiol.* 52, 607–624.
- Augustine, G.J., and Neher, E. (1992). Calcium requirements for secretion in bovine chromaffin cells. *J. Physiol.* 450, 247–271.
- Augustine, G.J., Charlton, M.P., and Smith, S.J. (1985). Calcium entry and transmitter release at voltage-clamped nerve terminals of squid. *J. Physiol.* 367, 163–181.
- Bruns, D., and Jahn, R. (1995). Real-time measurement of transmitter release from single synaptic vesicles. *Nature* 377, 62–65.
- Burgoyne, R.D. (1995). Fast exocytosis and endocytosis triggered by depolarization in single adrenal chromaffin cells before rapid  $\text{Ca}^{2+}$  current run-down. *Pflügers Arch.* 430, 213–219.
- Chow, R.H., and von Rüden, L. (1995). Electrochemical detection of secretion from single cells. In *Single-Channel Recording*, 2nd Ed., B. Sakmann and E. Neher, eds. (New York: Plenum Press), pp. 245–275.
- Chow, R.H., von Rüden, L., and Neher, E. (1992). Delay in vesicle fusion revealed by electrochemical monitoring of single secretory events in adrenal chromaffin cells. *Nature* 356, 60–63.
- Chow, R.H., Klingauf, J., and Neher, E. (1994). Time course of  $\text{Ca}^{2+}$  concentration triggering exocytosis in neuroendocrine cells. *Proc. Natl. Acad. Sci. USA* 91, 12765–12769.
- Coupland, R.E. (1968). Determining sizes and distribution of sizes of spherical bodies such as chromaffin granules in tissue sections. *Nature* 217, 384–388.
- de Camilli, P., and Jahn, R. (1990). Pathways to regulated exocytosis in neurons. *Annu. Rev. Physiol.* 52, 625–645.
- Douglas, W.W. (1968). Stimulus-secretion coupling: the concept and clues from chromaffin and other cells. *Brit. J. Pharmacol.* 34, 453–474.
- Hamill, O.P., Marty, A., Neher, E., Sakmann, B., and Sigworth, F. (1981). Improved patch clamp techniques for high-resolution current recording from cells and cell-free membrane patches. *Pflügers Arch.* 397, 85–100.
- Heinemann, C., Chow, R.H., Neher, E., and Zucker, R.S. (1994). Kinetics of the secretory response in bovine chromaffin cells following flash photolysis of caged  $\text{Ca}^{2+}$ . *Biophys. J.* 67, 2546–2557.
- Horrigan, F.T., and Bookman, R.J. (1994). Releaseable pools and the kinetics of exocytosis in adreanal chromaffin cells. *Neuron* 13, 1119–1129.
- Katz, B. (1969). *The Release of Neural Transmitter Substances*. (Liverpool, UK: Liverpool University Press).
- Lindau, M., and Neher, E. (1988). Patch-clamp techniques for time-resolved capacitance measurements in single cells. *Pflügers Arch.* 411, 137–146.
- Neher, E., and Augustine, G.J. (1992). Calcium gradients and buffers in bovine chromaffin cells. *J. Physiol.* 450, 273–301.
- Neher, E., and Marty, A. (1982). Discrete changes of cell membrane capacitance observed under conditions of enhanced secretion in bovine adrenal chromaffin cells. *Proc. Natl. Acad. Sci. USA* 79, 6712–6716.
- Neher, E., and Zucker, R.S. (1993). Multiple calcium-dependent processes related to secretion in bovine chromaffin cells. *Neuron* 10, 21–30.
- Nowycky, M.C., and Pinter, M.J. (1993). Time courses of calcium and calcium-bound buffers following calcium influx in a model cell. *Biophys. J.* 64, 77–91.
- Roberts, W.M. (1994). Localization of calcium signals by a mobile calcium buffer in frog saccular hair cells. *J. Neurosci.* 14, 3246–3262.
- Thomas, P., Lee, A.K., Wong, J.G., and Almers, W. (1994). A triggered mechanism retrieves membrane in seconds after  $\text{Ca}^{2+}$ -stimulated exocytosis in single pituitary cells. *J. Cell Biol.* 124, 667–675.
- Verhage, M., McMahon, H.T., Ghijsen, W.E.J.M., Boomsma, F., Scholten, G., Wiegant, V.M., and Nicholls, D.G. (1991). Differential release of amino acids, neuropeptides, and catecholamines from isolated nerve terminals. *Neuron* 6, 517–524.
- von Rüden, L., and Neher, E. (1993). A Ca-dependent step in the release of catecholamines from adrenal chromaffin cells. *Science* 262, 1061–1065.
- Yamada, W.M., and Zucker, R.S. (1992). Time course of transmitter release calculated from simulations of a calcium diffusion model. *Biophys. J.* 61, 671–682.
- Zhou, Z., and Misler, S. (1995). Action potential-induced quantal secretion of catecholamines from rat adrenal chromaffin cells. *J. Biol. Chem.* 270, 3498–3505.
- Zhou, Z., and Neher, E. (1993). Mobile and immobile calcium buffers in bovine adrenal chromaffin cells. *J. Physiol.* 469, 245–273.